Local Effects of Sheared Grazing Flow on Impedance Eduction

Lucas A. Bonomo*,
Federal University of Santa Catarina, 88040-900 Florianópolis, Brazil
University of Warwick, Coventry CV4 7AL, United Kingdom

Edward J. Brambley†,
University of Warwick, Coventry CV4 7AL, United Kingdom

Nicolas T. Quintino‡, Lucas M. Pereira§, Julio A. Cordioli¶,
Federal University of Santa Catarina, 88040-900 Florianópolis, Brazil

Francesco Avallone‖
Politecnico di Torino, 10129, Torino, Italy

Impedance eduction is the preferred method for acoustic liner characterization under grazing flow conditions. The method usually assumes an uniform impedance for the whole lined wall. However, in situ local measurements suggest the liner impedance is influenced by the flow profile above the liner. Therefore, the liner impedance is expected to vary spatially due to the three-dimensional nature of the grazing flow profile inside dedicated test rigs. In this work, we study the impact on impedance eduction of failing to account for this local variation in liner impedance. A numerical synthesized experiment is used to investigate the uniform impedance assumption. The axial wavenumbers of a lined rectangular duct with sheared flow profile are obtained by solving the Pridmore-Brown Equation. The wavenumbers in the lined section are evaluated with both a variable wall impedance and with the wall impedance taken constant at an averaged value. The wavenumbers are then used to educe the lined wall impedance by means of the traditional straightforward impedance eduction method. Results suggest that the impact of assuming an uniform impedance at the lined wall are negligible, since both upstream and downstream wavenumbers evaluated for the different impedance assumptions almost perfectly match.

I. Introduction

Acoustic liners are passive devices applied to the walls of aircraft engine nacelles to mitigate fan noise. Typically, these liners consist of a honeycomb structure sandwiched between a hard backplate and a perforated facesheet. They are conventionally modeled using a locally-reacting acoustic impedance, a frequency-dependent complex property. This impedance is known to depend on liner geometry [1, 2] and operational conditions, such as Sound Pressure Level (SPL) [3] and the grazing flow velocity [1] and profile [4] over the liner surface.

For characterizing acoustic liners with grazing flow, the liner community has relied on either the in-situ technique (or Dean's method) [5] or impedance eduction methods [6–8]. The former involves measuring the acoustic field on both the facesheet and the backplate of a liner cell using miniaturized microphones or microphone probes. On the other hand, impedance eduction techniques rely on measuring the in-duct acoustic field on dedicated test rigs: from a duct acoustic propagation model, the acoustic liner impedance seen by the acoustic field is obtained. While the in-situ technique provides a local value of the liner impedance, impedance eduction techniques evaluate an averaged effect over the whole liner. Due to its simpler instrumentation, higher repeatability, and applicability to different liner constructions, impedance eduction is generally preferred over the earlier in-situ technique [9, 10].

---

*Visiting Researcher PhD Student, Warwick Mathematics Institute, lucas.bonomo@lva.ufsc.br, AIAA Student Member.

†Reader (Associate Professor), Warwick Mathematics Institute and WMG, E.J.Brambley@warwick.ac.uk, AIAA Senior Member.

‡MSc Student, Laboratory of Vibration and Acoustics, nicolas.quintino@lva.ufsc.br, AIAA Student Member.

§PhD Student, Laboratory of Vibration and Acoustics, lucas.meirelles@lva.ufsc.br, AIAA Student Member.

¶Associate Professor, Department of Mechanical Engineering, julio.cordioli@ufsc.br, AIAA Member.

‖Full Professor, Department of Mechanical and Aerospace Engineering, francesco.avallone@polito.it, AIAA Member.

In principle, the acoustic impedance of liners should remain independent of the incident acoustic field (locally reactive assumption). However, recent evidence has shown a discrepancy when the wave propagation direction changes between upstream- and downstream-propagating waves, suggesting flaws in the modeling used for impedance eduction [11–14]. Most impedance eduction methods rely on a duct propagation model, with uniform flow and the Ingard-Myers boundary condition as common assumptions. Several attempts have been made to include governing equations capturing actual liner physics. For instance, Weng et al. [15] found that viscosity is unable to account for the discrepancy between upstream and downstream and collapse the educed impedances. Nark et al. [16] found that small changes to the mean flow velocity were able to reduce the gap between the upstream and downstream educed impedances. Roncen et al. [17] showed that the inconsistency persists even when considering a three-dimensional inviscid sheared flow profile and a no-slip condition at the lined wall, suggesting that liner physics are not fully captured. Novel boundary conditions have been introduced to better describe liner physics, but none have accurately predicted acoustic wavenumbers when the experimental configuration is changed, as concluded by Spillere et al. [18].

The acoustic impedance of traditional single-degree-of-freedom acoustic liners is known to depend not only on the bulk Mach number but also on the sheared flow profile of the grazing flow over the perforated facesheet [4]. Dedicated test rigs for acoustic liner characterization typically use rectangular cross-sectional ducts, which implies that the internal flow profile has a three-dimensional nature. With this in mind, the acoustic impedance of liners is expected to vary spatially within the test rigs, considering that each cell faces a different mean flow velocity gradient. However, impedance eduction techniques generally assume a uniform impedance for the entire liner sample. A notable exception is the work of Roncen et al. [19], which proposed an impedance eduction method that takes into account the spatial variation of impedance due to the SPL variation over the wall. It was found that the direction of the flow relative to the incident wave propagation seems to play a role in the space-dependency of the impedance. If the variation of impedance with SPL is neglected, the educed value of the impedance was found to depend on the length of the liner. However, the influence of SPL on liner impedance is expected to be significantly smaller than the effect of variations of the grazing flow considered here, especially for higher flow velocities [3, 10].

In this work, our primary focus is to investigate the potential effects of the spatially varying impedance due to the flow profile variation in the liner's transverse direction. A numerical experiment is proposed to synthesize the axial wavenumbers in a lined duct with sheared flow and a variable impedance at the wall. The wavenumbers for the spatially variable impedance are compared to the wavenumbers obtained for an averaged impedance. Then, the traditional straightforward impedance eduction [7] is used to analyze the impact of the variable impedance in the eduction results.

This work is organized as follows. The governing equations and the numerical method for solving the resulting eigenvalue problem are discussed in Section II. The spatial dependence model assumed for the liner is described in Section III. The numerical experiment used to synthesized data for the impedance eduction is described in Section IV. The results are presented in Section V, while the main conclusions are outlined in Section VI.

II. Governing Equations

For the purpose of this study, the infinite rectangular duct depicted in Fig. 1 can be considered. The duct cross-section has width W and height H. An axial flow with flow profile $\mathbf{u}_0 = U_0(x, y)\mathbf{e_z}$ is assumed. This implies that both the flow profile and the impedance have no dependence on the axial direction. The wall located at $x = -W/2$ has a locally-reacting spatial- and frequency-dependent impedance $Z(\omega, y)$, while all the other walls are acoustically rigid.

For the purpose of this work, we will assume that the in-duct acoustic propagation can be described by the Pridmore-Brown Equation (PBE) [20], such that

$$(i\omega + \mathbf{u}_0 \cdot \nabla)\left(\frac{1}{c_0^2}(i\omega + \mathbf{u}_0 \cdot \nabla)^2 \tilde{p}' - \nabla^2 \tilde{p}'\right) + 2\frac{\partial}{\partial z}\left(\nabla \tilde{p}' \cdot \nabla U_0\right) = 0, \tag{1}$$

where $\tilde{p}'$ is the acoustic pressure with assumed monochromatic time dependence $\exp\{i\omega t\}$, c_0 the speed of sound, $i = \sqrt{-1}$ the complex imaginary unity and $\nabla = (\partial/\partial x, \partial/\partial y, \partial/\partial z)$. Considering the axial invariance of the problem, we assume an axial dependence on the form $\tilde{p}'(x, y, z) = \tilde{p}'(x, y)\exp\{-ik_z z\}$, where k_z is the axial wavenumber, so Eq. (1) can be written as

$$\left(\nabla_\perp^2 + \frac{\omega^2}{c_0^2}\right)\tilde{p}' - k_z\left(\frac{U_0}{\omega}\nabla_\perp^2 - \frac{2}{\omega}\nabla_\perp U_0 \cdot \nabla_\perp + \frac{3\omega U_0}{c_0^2}\right)\tilde{p}' - k_z^2\left(1 - \frac{3U_0^2}{c_0^2}\right)\tilde{p}' - k_z^3\left[\frac{U_0}{\omega}\left(\frac{U_0^2}{c_0^2} - 1\right)\right]\tilde{p}' = 0, \tag{2}$$
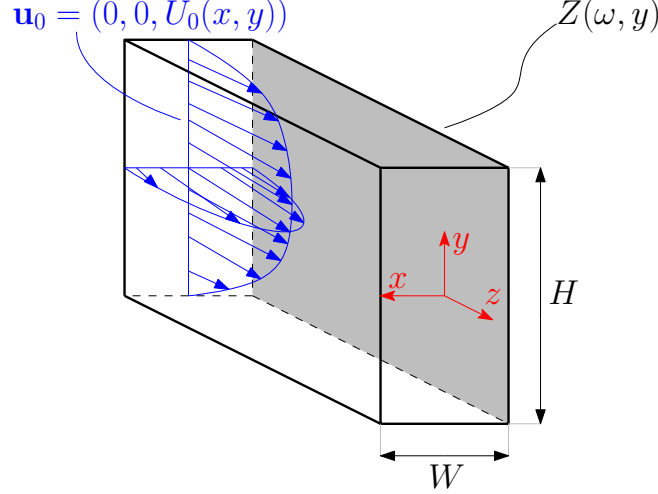
Fig. 1   Schematic duct and coordinates system assumed in this work.

where $\nabla_\perp = (\partial/\partial x, \partial/\partial y, 0)$. As boundary conditions, at rigid walls, the normal acoustic velocity $\mathbf{u}'$ vanishes, such that

$$\mathbf{u}' \cdot \hat{n} = 0, \tag{3}$$

where $\hat{n}$ is a unitary normal vector pointing into the wall. Non-slip flows are assumed, therefore the locally reacting impedance boundary condition can be written as

$$Z = \frac{1}{\rho_0 c_0} \frac{\tilde{p}'}{\mathbf{u}' \cdot \hat{n}}, \tag{4}$$

where the air characteristic impedance $\rho_0 c_0$ is used as a normalization factor and ρ_0 is the air density.

A. Uniform Flow Case

If a uniform flow is assumed, i.e., $U_0 \equiv M c_0 = $ constant, where M is the bulk (average) Mach number, the PBE reduces to the Convected Helmholtz Equation (CHE),

$$\nabla^2 \tilde{p}' + \left(k_0 - iM \frac{\partial}{\partial z} \right)^2 \tilde{p}' = 0. \tag{5}$$

where $k_0 \equiv \omega/c_0$ is the free-field wavenumber.

The impedance boundary condition, given by Eq. (4), is valid provided the mean flow velocity vanishes at the wall. With a uniform flow model, such as the CHE, the flow velocity adjacent to the wall is non-zero, although in reality there is a thin boundary layer at the wall. The refractive effects that occur within this thin boundary layer must then be taken into account by the boundary condition. The most common assumption used is the so-called Ingard–Myers Boundary Condition (IMBC) [21, 22], which can be written as

$$Z_{\text{eff,IMBC}} = \frac{1}{\rho_0 c_0} \frac{\tilde{p}'}{\mathbf{u}' \cdot \hat{n}} = \frac{\omega Z}{\omega - c_0 M k_z}. \tag{6}$$

B. Numerical Scheme

We seek to describe the governing equations as a generalized eigenvalue problem. One can rewrite the PBE (Eq. (2)) as

$$(A_0 + A_1 k_z + A_2 k_z^2 + A_3 k_z^3) \tilde{\mathbf{p}}' = \mathbf{0}, \tag{7}$$

where the A_j terms involve differentiation in x and y and multiplication by the frequency ω, by the mean flow U_0 and by its x- and y-derivatives and $\tilde{\mathbf{p}}'$ the discretized acoustic pressure. In the present work, we follow a strategy similar

3

to Boyer et al. [23], where the problem is discretized by projecting it onto a Gauss–Lobatto grid using Chebyshev polynomials as basis. Finally, to solve the cubic generalized eigenvalue problem given by Eq. (7), auxiliary variables are introduced of the form $\tilde{\mathbf{p}}_p = k_z \tilde{\mathbf{p}}_{p-1}$ for $p > 0$ [24, p. 129], and the resulting sparse linear eigenvalue problem is solved using the `eigs` function from MATLAB.

In order to apply a lined wall boundary condition to the generalized eigenvalue problem, we rewrite Eq. (4) as

$$\frac{\mathrm{d}\tilde{p}'}{\mathrm{d}x}n_x + \frac{\mathrm{i}\omega}{Z}\tilde{p}' = 0, \tag{8}$$

where $n_x = -1$ at $x = -W/2$. For the hard wall opposite to the liner, the corresponding boundary condition is

$$\frac{\mathrm{d}\tilde{p}'}{\mathrm{d}x} = 0. \tag{9}$$

Similarly, for the hard walls at $y = \pm H/2$, one may write

$$\frac{\mathrm{d}\tilde{p}'}{\mathrm{d}y} = 0. \tag{10}$$

III. Impedance Spatial Dependence

The definition of the impedance spatial dependence is a key point of this study. In this work, we use the non-linear flow term from the well-known Goodrich model [25], that gives the impedance

$$Z(\omega, y) = R(\omega) + R_{cm}(y) + \mathrm{i}X(\omega), \tag{11}$$

where $R(\omega)$ is the *linear* component of the liner resistance, $X(\omega)$ is the liner reactance and

$$R_{cm}(y) = \frac{M(y)}{\sigma\left(2 + 1.256\dfrac{\delta^*(y)}{d}\right)}. \tag{12}$$

Here, M is the free-stream Mach number, σ the open area ratio of the liner, δ^* the boundary layer displacement thickness and d the perforate plate holes diameter. One may notice that, in this study, the variables M and δ^* are evaluated only for the flow profile immediately above the liner. Also, by assuming the Goodrich model as reference for the flow effect, the reactance is taken to be uniform over the whole lined wall.

IV. Numerical Experiment

In this study, a numeric synthesized experiment is used to estimate the impact of the local variations of the impedance due to the 2D flow profile. The procedure can be summarized as follows.

The PBE eigenvalue solver described in Section II.B is used to evaluate the axial wavenumbers in the lined duct with sheared grazing flow. This can be compared to a real world impedance eduction method where the wavenumbers are extracted from an equally-spaced acoustic pressure sampling by means of Prony-like algorithms. Two pairs of wavenumbers are considered: (I) $k_z^{\pm}(Z(y))$, determined for the case with the impedance spatially varying, and; (II) $k_z^{\pm}(\langle Z(y)\rangle)$, which corresponds to the case where the *spatial average* of the impedance is uniformly applied to the lined wall. The superscript + denotes downstream propagation, while − denotes upstream propagation (upstream and downstream sources, respectively). Both upstream and downstream propagating modes wavenumbers are obtained, *considering the same impedance for both directions*.

The axial wavenumbers thus obtained are then used for traditional straightforward impedance eduction [7]. This procedure consists of applying the Ingard–Myers boundary condition to the CHE solution, assuming the lined wall impedance is uniform, which leads to the eigenvalue problem

$$\alpha \tan(\alpha W/2) - \frac{\rho_0 c_0}{\mathrm{i}k_0 Z}(\mathrm{i}k - \mathrm{i}Mk_z)^2 = 0, \tag{13}$$

where α are the transverse wavenumbers, and with the dispersion relation given by

$$\alpha^2 = (k_0 - Mk_z)^2 - k_z^2, \tag{14}$$

one is able to obtain the liner impedance. This procedure is done independently for the two different propagating directions.

The test conditions are described in what follows. The numerical experiment replicates the UFSC Liner Test Rig geometry. The computational domain represents a rectangular duct of dimensions $H = 100$ mm and $W = 40$ mm. For the numerical experiment, the bulk Mach number is set to 0.3. The typical frequency range from 500 to 3000 Hz is considered.

The stream-wise flow profile in the midspan of both normal-wise, $U_x(x)$, and transverse-wise, $U_y(y)$, directions ($y = 0$ and $x = 0$, respectively) are described by a modified Universal-Wall Law, which can be written for the three boundary layer sublayers as

$$\text{Viscous sublayer } 0 \le \xi^+ < 5 \qquad u^+ = \xi^+, \tag{15a}$$

$$\text{Buffer sublayer } 5 \le \xi^+ < 70 \qquad u^+ = \frac{1}{\Lambda}\left[\frac{1}{3}\ln\frac{\Lambda\xi^+ + 1}{\sqrt{(\Lambda\xi^+)^2 - \Lambda\xi^+ + 1}} + \frac{1}{\sqrt{3}}\left(\tan^{-1}\frac{2\Lambda\xi^+ - 1}{\sqrt{3}} + \frac{\pi}{6}\right)\right]$$
$$+ \frac{1}{4\kappa}\ln(1 + \kappa B\xi^{+4}), \tag{15b}$$

$$\text{Overlap sublayer } 70 \le \xi^+ \qquad u^+ = \frac{1}{\kappa}\ln\xi^+ + C^+ + \frac{1}{\kappa\xi_c^+}(\xi_c^+ - \xi^+)\left(\frac{\xi^+}{\xi_c^+}\right)^2, \tag{15c}$$

where $\xi^+ = \xi u_\tau/\nu$, with ξ the distance to the wall*, u_τ the friction velocity and ν the fluid kinematic viscosity, $u^+ = U/u_\tau$, with U the dimensional streamwise velocity. The other variables are the von Kármán constant, $\kappa = 0.41$ and

$$\Lambda = (A + B)^{(1/3)}, \quad A = 6.1 \times 10^{-4}, \quad B = 1.43 \times 10^{-3}.$$

The last term on the right-hand side of the overlap sublayer equation (Eq. (15c)) was included such that the derivative of the profile is continuous at the duct centreline. This results in a slight different matching constant $C^+ = 4.946$. In this work, the friction velocities for the flow profiles U_x and U_y, are $u_\tau^x = 3.967$ m s^{-1} and $u_\tau^y = 3.733$ m s^{-1}, respectively. These values were determined by fitting the modified Universal-Wall Law to the flow profile experimentally measured at the UFSC test rig for a bulk Mach number of 0.3. The two 1D flow profiles are tensorized to a 2D flow profile and rescaled for the bulk Mach number by

$$\frac{U_0(x, y)}{c_0} = M\frac{U_x(x)}{\langle U_x(x)\rangle}\frac{U_y(y)}{\langle U_y(y)\rangle}, \tag{16}$$

where the operator $\langle\cdot\rangle$ denotes averaging over the function domain. One may notice that for this choice of flow profile representation, the boundary layer displacement thickness is constant along the $y-$axis, i;e. $\delta^*(y) = $ cte..

For the current numerical synthetic study, the impedance predict by the Goodrich impedance model for a typical single-degree-of-freedom liner sample is used. The considered liner geometry corresponds to the 3D-printed liner sample which has been extensively used by the authors in previous (and ongoing) experimental and high-fidelity simulation investigations [26, 27]. The perforate facesheet has holes with diameter of 1.17 mm, thickness of 0.55 mm and a percentage of open area of approximately 8.8 %[†] The reference impedance is shown in Fig. 2, with the linear component of the resistance, $R(\omega)$ and the spatial average of the variable impedance

$$\langle R(\omega) + R_{cm}(y)\rangle = R(\omega) + \frac{1}{H}\int_{-H/2}^{H/2} R_{cm}(y)\mathrm{d}y, \tag{17}$$

shown in Fig. 2a, while the variable component of the resistance is shown in Fig. 2b.

---

*For $U_x(x)$, $\xi = W/2 - |x|$, while for $U_y(y)$, $\xi = H/2 - |y|$.

[†]These values diverges significantly from the nominal ones presented in previous publications. This new set of parameters was obtained through a 3D-scanning procedure that is going to be described in a companion paper.
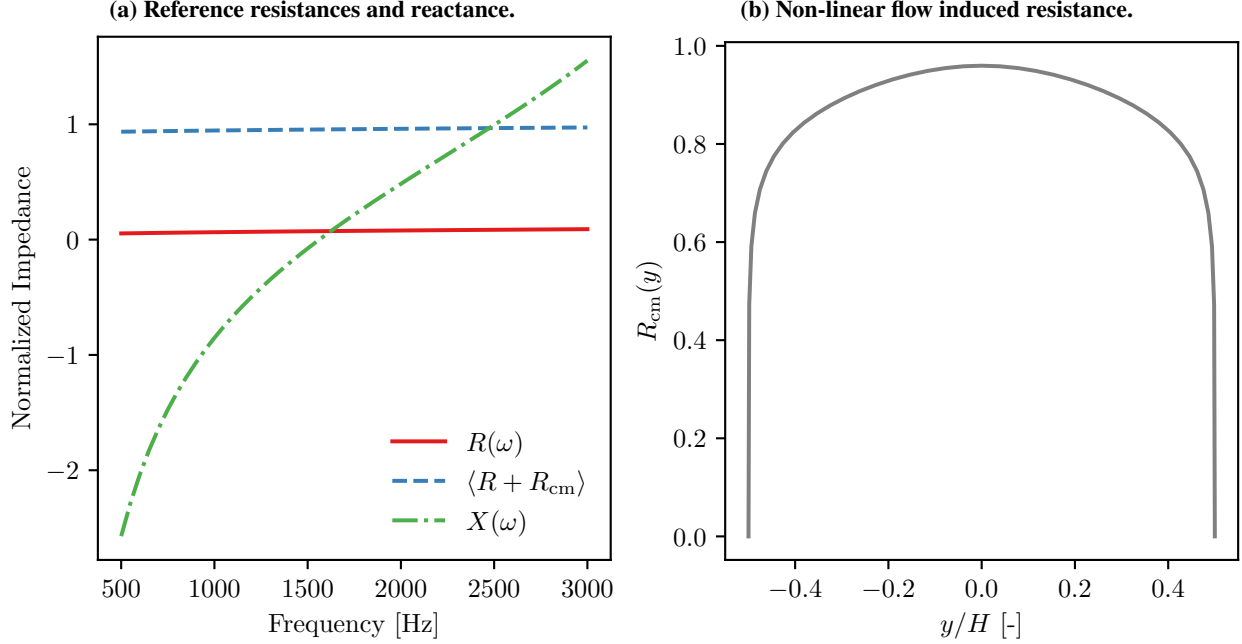
| (a) Reference resistances and reactance. | (b) Non-linear flow induced resistance. |

Fig. 2   Reference impedances for the numeric experiment.

V. Results

The reference axial wavenumbers evaluated for both variable impedance and spatially-averaged uniform impedance are shown in Fig. 3. The curves for both cases almost perfectly collapses, with just small differences observed near the liner resonance, as highlighted in the imaginary component plots. Results suggest that the impedance averaging slightly underestimates the absolute value of the axial wavenumber when compared to the variable impedance case. This match anticipates that the impedance spatially dependence may not significantly impact the impedance eduction.

The wavenumbers obtained for both variable impedance, $Z_{\mathrm{ref}}(y)$ and the averaged impedance $\langle Z_{\mathrm{ref}}(y)\rangle$ are then used in the traditional straightforward impedance eduction method. The impedances obtained for both approaches for both Upstream Source (US) and Downstream Sources (DS) are shown in Fig. 4. For the reactances, a perfect match is observed between the two approaches. For the resistances, small differences are observed, especially for the downstream source, although the differences are almost negligible, as the similar wavenumbers already suggest. The typical mismatch between upstream and downstream acoustic sources observed in experimental eduction is also noticed in the results. The fact that the mismatch was still observed, even though the wavenumbers were synthesized from the same reference impedance in this case, can be explained by the bias error induced by the uniform flow assumption with the Ingard-Myers boundary condition when compared to the reference 2D-PBE, as suggested by Roncen et al. [17].

VI. Concluding Remarks

In this work, a numerical synthesized experiment was used to study the impact of a spatially varying impedance in the lined wall of rectangular ducts due to the varying sheared flow profile. The synthetic experiment was performed by solving the 2D Pridmore-Brown Equation, considering a sheared flow profile and a variable impedance dependent on the transverse direction. The wavenumbers obtained for the variable impedance configuration were compared with the ones evaluated for an averaged impedance. Later, the wavenumbers obtained for both assumptions were used in a traditional impedance eduction procedure. Results obtained suggest that the acoustic field perceives an effective impedance that corresponds to the spatial average of the variable impedance wall. The wavenumbers predicted for both configurations almost perfectly match, and the educed impedance obtained with the wavenumbers for the different cases collapses into a single curve. The bias error induced by assuming an uniform flow and the Ingard–Myers boundary condition is observed, as already documented in the literature [17, 28]. In summary, this study suggests the impact of assuming an uniform impedance at the lined wall, even though a variation is expected in the transversal direction, may be negligible.
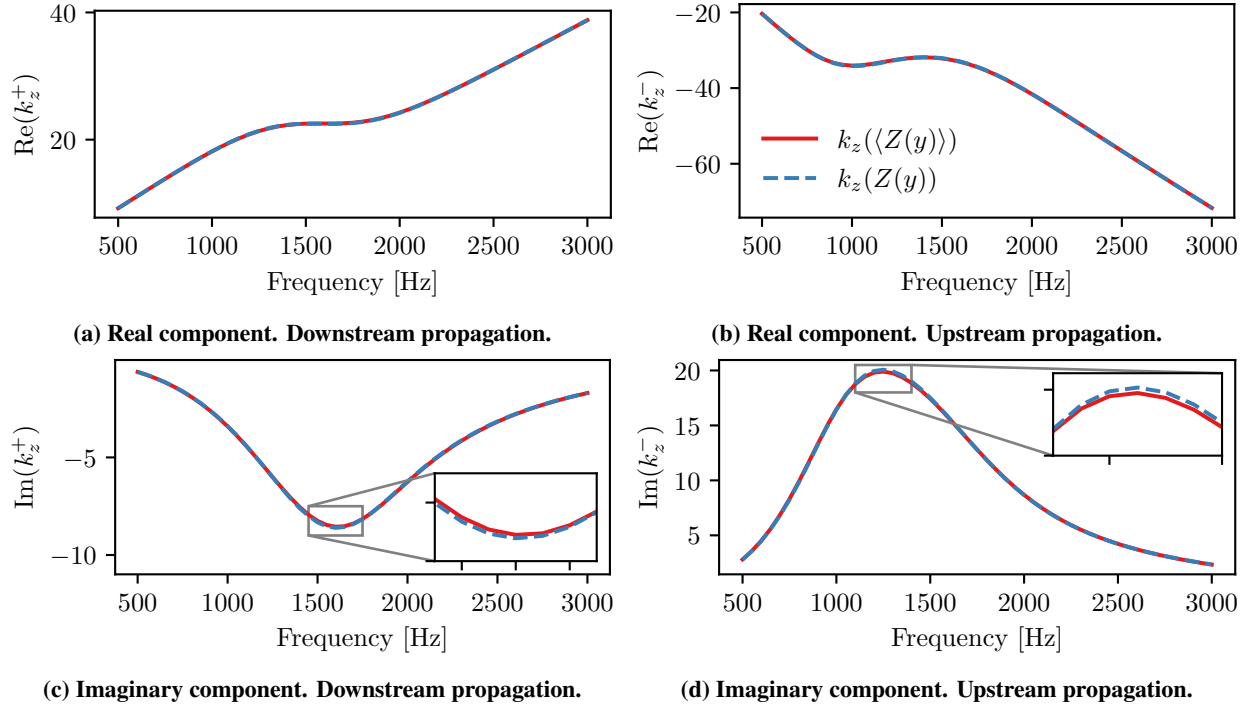
6

(a) Real component. Downstream propagation.

(b) Real component. Upstream propagation.

(c) Imaginary component. Downstream propagation.

(d) Imaginary component. Upstream propagation.

Fig. 3 Reference wavenumbers. Evaluated by solving the PBE eigenvalue problem for both the variable impedance at the lined wall and the spatially-averaged uniform impedance cases.
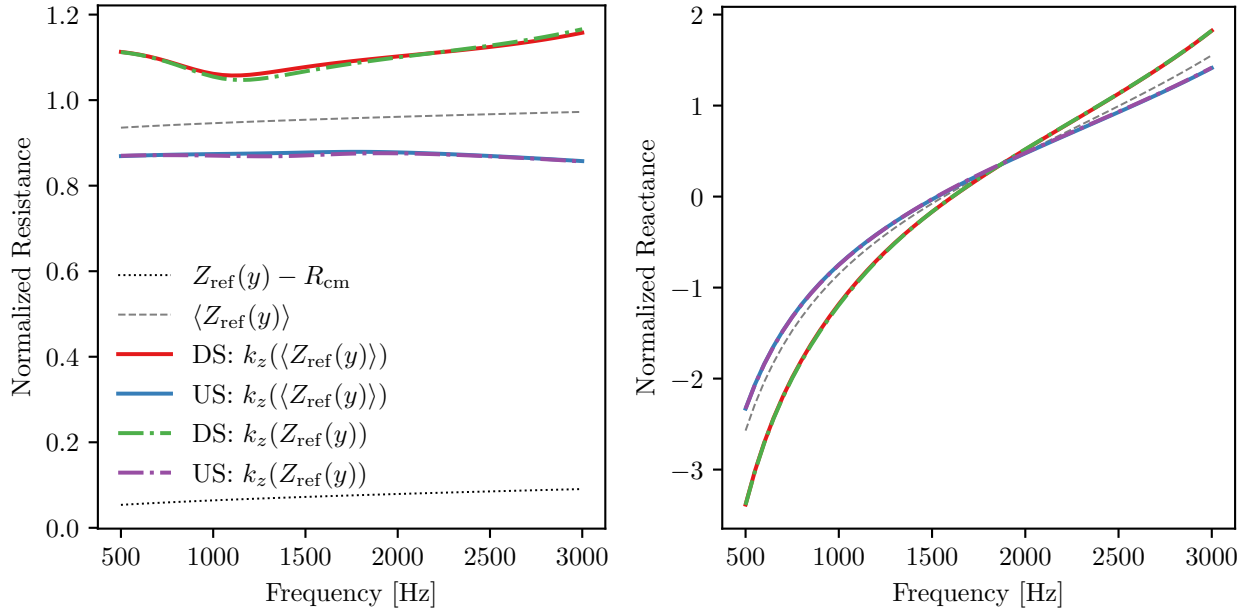

Fig. 4 Educed impedances obtained with numerical synthesized wavenumbers. DS: Downstream Source (upstream propagation); US: Upstream Source (downstream propagation).

Acknowledgments

References

[1] Guess, A. W., "Calculation of Perforated Plate Liner Parameters from Specified Acoustic Resistance and Reactance," *Journal of Sound and Vibration*, Vol. 40, No. 1, 1975, pp. 119–137. https://doi.org/10.1016/S0022-460X(75)80234-3.

[2] Jones, M., Tracy, M., Watson, W., and Parrott, T., "Effects of Liner Geometry on Acoustic Impedance," *8th AIAA/CEAS Aeroacoustics Conference & Exhibit*, American Institute of Aeronautics and Astronautics, Breckenridge, Colorado, 2002. https://doi.org/10.2514/6.2002-2446.

[3] Murray, P., and Astley, R. J., "Development of a Single Degree of Freedom Perforate Impedance Model under Grazing Flow and High SPL," *18th AIAA/CEAS Aeroacoustics Conference (33rd AIAA Aeroacoustics Conference)*, American Institute of Aeronautics and Astronautics, Colorado Springs, Colorado, 2012. https://doi.org/10.2514/6.2012-2294.

[4] Kooi, J., and Sarin, S., "An Experimental Study of the Acoustic Impedance of Helmholtz Resonator Arrays under a Turbulent Boundary Layer," *7th Aeroacoustics Conference*, American Institute of Aeronautics and Astronautics (AIAA), Palo Alto,CA,U.S.A., 1981. https://doi.org/10.2514/6.1981-1998.

[5] Dean, P., "An in Situ Method of Wall Acoustic Impedance Measurement in Flow Ducts," *Journal of Sound and Vibration*, Vol. 34, No. 1, 1974, pp. 97–IN6. https://doi.org/10.1016/S0022-460X(74)80357-3.

[6] Watson, W., Jones, M., and Parrott, T., "Validation of an Impedance Eduction Method in Flow," *AIAA Journal*, Vol. 37, No. 7, 1999, pp. 818–824. https://doi.org/10.2514/2.7529.

[7] Jing, X., Peng, S., and Sun, X., "A Straightforward Method for Wall Impedance Eduction in a Flow Duct," *The Journal of the Acoustical Society of America*, Vol. 124, No. 1, 2008, pp. 227–234. https://doi.org/10.1121/1.2932256.

[8] Elnady, T., Bodén, H., and Elhadidi, B., "Validation of an Inverse Semi-Analytical Technique to Educe Liner Impedance," *AIAA Journal*, Vol. 47, No. 12, 2009, pp. 2836–2844. https://doi.org/10.2514/1.41647.

[9] Ferrante, P., De Roeck, W., Desmet, W., and Magnino, N., "Back-to-Back Comparison of Impedance Measurement Techniques Applied to the Characterization of Aero-Engine Nacelle Acoustic Liners," *Applied Acoustics*, Vol. 105, 2016, pp. 129–142. https://doi.org/10.1016/j.apacoust.2015.12.004.

[10] Bonomo, L. A., Quintino, N. T., Spillere, A., Cordioli, J. A., and Murray, P. B., "A Comparison of In-Situ and Impedance Eduction Experimental Techniques for Acoustic Liners with Grazing Flow and High SPL," *28th AIAA/CEAS Aeroacoustics 2022 Conference*, American Institute of Aeronautics and Astronautics, 2022. https://doi.org/10.2514/6.2022-2998.

[11] Renou, Y., and Aurégan, Y., "Failure of the Ingard–Myers Boundary Condition for a Lined Duct: An Experimental Investigation," *The Journal of the Acoustical Society of America*, Vol. 130, No. 1, 2011, p. 52. https://doi.org/10.1121/1.3586789.

[12] Bodén, H., Zhou, L., Cordioli, J. A., Medeiros, A. A., and Spillere, A. M., "On the Effect of Flow Direction on Impedance Eduction Results," *22nd AIAA/CEAS Aeroacoustics Conference, 2016*, American Institute of Aeronautics and Astronautics Inc, AIAA, Lyon, France, 2016. https://doi.org/10.2514/6.2016-2727.

[13] Roncen, R., Piot, E., Mery, F., Simon, F., Jones, M. G., and Nark, D. M., "Influence of Source Propagation Direction and Shear Flow Profile in Impedance Eduction of Acoustic Liners," *25th AIAA/CEAS Aeroacoustics Conference*, American Institute of Aeronautics and Astronautics, Delft, The Netherlands, 2019. https://doi.org/10.2514/6.2019-2469.

[14] Bodén, H., Cordioli, J. A., Spillere, A. M., and Serrano, P. G., "Comparison of the Effect of Flow Direction on Liner Impedance Using Different Measurement Methods," *23rd AIAA/CEAS Aeroacoustics Conference, 2017*, American Institute of Aeronautics and Astronautics Inc, AIAA, Denver, Colorado, 2017. https://doi.org/10.2514/6.2017-3184.

[15] Weng, C., Schulz, A., Ronneberger, D., Enghardt, L., and Bake, F., "Flow and Viscous Effects on Impedance Eduction," *AIAA Journal*, Vol. 56, No. 3, 2018, pp. 1118–1132. https://doi.org/10.2514/1.J055838.

[16] Nark, D. M., Jones, M. G., and Piot, E., "Assessment of Axial Wave Number and Mean Flow Uncertainty on Acoustic Liner Impedance Eduction," *2018 AIAA/CEAS Aeroacoustics Conference*, American Institute of Aeronautics and Astronautics, Reston, Virginia, 2018. https://doi.org/10.2514/6.2018-3444.

[17] Roncen, R., Piot, E., Méry, F., Simon, F., Jones, M. G., and Nark, D. M., "Wavenumber-Based Impedance Eduction with a Shear Grazing Flow," *AIAA Journal*, Vol. 58, No. 7, 2020, pp. 3040–3050. https://doi.org/10.2514/1.J059100.

[18] Spillere, A. M. N., Bonomo, L. A., Cordioli, J. A., and Brambley, E. J., "Experimentally Testing Impedance Boundary Conditions for Acoustic Liners with Flow: Beyond Upstream and Downstream," *Journal of Sound and Vibration*, Vol. 489, 2020, p. 115676. https://doi.org/10.1016/J.JSV.2020.115676.

[19] Roncen, R., Méry, F., Piot, E., and Klotz, P., "Spatially-Varying Impedance Model for Locally Reacting Acoustic Liners at a High Sound Intensity," *Journal of Sound and Vibration*, Vol. 524, 2022, p. 116741. https://doi.org/10.1016/j.jsv.2021.116741.

[20] Pridmore-Brown, D. C., "Sound Propagation in a Fluid Flowing through an Attenuating Duct," *Journal of Fluid Mechanics*, Vol. 4, No. 04, 1958, pp. 393–406. https://doi.org/10.1017/S0022112058000537.

[21] Ingard, U., "Influence of Fluid Motion Past a Plane Boundary on Sound Reflection, Absorption, and Transmission," *The Journal of the Acoustical Society of America*, Vol. 31, No. 7, 1959, pp. 1035–1036. https://doi.org/10.1121/1.1907805.

[22] Myers, M. K., "On the Acoustic Boundary Condition in the Presence of Flow," *Journal of Sound and Vibration*, Vol. 71, 1980, pp. 429–434. https://doi.org/10.1016/0022-460X(80)90424-1.

[23] Boyer, G., Piot, E., and Brazier, J.-P., "Theoretical Investigation of Hydrodynamic Surface Mode in a Lined Duct with Sheared Flow and Comparison with Experiment," *Journal of Sound and Vibration*, Vol. 330, No. 8, 2011, pp. 1793–1809. https://doi.org/10.1016/j.jsv.2010.10.035.

[24] Boyd, J., *Chebyshev and Fourier Spectral Methods*, 2nd ed., Dover Books on Mathematics, Dover Publications, 2001.

[25] Yu, J., Ruiz, M., and Kwan, H. W., "Validation of Goodrich Perforate Liner Impedance Model Using NASA Langley Test Data," *14th AIAA/CEAS Aeroacoustics Conference (29th AIAA Aeroacoustics Conference)*, Vancouver, British Columbia, Canada, 2008. https://doi.org/10.2514/6.2008-2930.

[26] Bonomo, L. A., Quintino, N. T., Cordioli, J. A., Avallone, F., Jones, M. G., Howerton, B. M., and Nark, D. M., "A Comparison of Impedance Eduction Test Rigs with Different Flow Profiles," *AIAA AVIATION 2023 Forum*, American Institute of Aeronautics and Astronautics, San Diego, CA, USA, 2023. https://doi.org/10.2514/6.2023-3346.

[27] Pereira, L., Bonomo, L., Quintino, N., da Silva, A., Cordioli, J., and Avallone, F., "Validation of High-Fidelity Numerical Simulations of Acoustic Liners Under Grazing Flow," *AIAA AVIATION 2023 FORUM*, San Diego, USA, 2023.

[28] Yang, J., Humbert, T., Golliard, J., and Gabard, G., "Shear flow effects in a 2D duct: Influence on wave propagation and direct impedance eduction," *Journal of Sound and Vibration*, Vol. 576, 2024, p. 118296.